Radio propagation measurements and modeling for standardization of the site general path loss model in International Telecommunications Union recommendations for 5G wireless networks

Radio Science

RESEARCH ARTICLE
10.1029/2019RS006924

Special Section:
RADIO CHANNEL MODELLING FOR 5G MILLIMETRE WAVE COMMUNICATIONS IN BUILT ENVIRONMENTS

Radio propagation measurements and modeling for standardization of the site general path loss model in International Telecommunications Union recommendations for 5G wireless networks

S. Salous[1], J. Lee[2], M. D. Kim[2], M. Sasaki[3], W. Yamada[3], X. Raimundo[1], and A. A. Cheema[1]

[1]Department of Engineering, Durham University, Durham, UK, [2]Telecommunications and Media Research Laboratory, ETRI, Daejeon, South Korea, [3]NTT Access Network Service Systems Laboratories, NTT Corporation, Tokyo, Japan

Key Points:
- Path loss model in the built environment for future wireless networks
- Impact of model coefficients on Monte Carlo simulation
- Site general models in ITU-R recommendations

Correspondence to:
S. Salous,
sana.salous@durham.ac.uk

Citation:
Salous, S., Lee, J., Kim, M. D., Sasaki, M., Yamada, W., Raimundo, X., & Cheema, A. A. (2020). Radio propagation measurements and modeling for standardization of the site general path loss model in International Telecommunications Union recommendations for 5G wireless networks. *Radio Science*, *55*, e2019RS006924. https://doi.org/10.1029/2019RS006924

Received 19 JUL 2019
Accepted 30 DEC 2019
Accepted article online 2 JAN 2020

Abstract The International Telecommunications Union Radiocommunication Sector (ITU-R) Study Group 3 identified the need for a number of radio channel models in anticipation of the World Radiocommunications Conference in 2019 when the frequency allocation for 5G will be discussed. In response to the call for propagation path loss models, members of the study group carried out measurements in the frequency bands between 0.8 GHz up to 73 GHz in urban low-rise and urban high-rise as well as suburban environments. The data were subsequently merged to generate site general path loss models. The paper presents an overview of the radio channel measurements, the measured environments, the data analysis, and the approach for the derivation of the path loss model adopted in Recommendation ITU-R P.1411-10 (2019-08).

Plain Language Summary Wireless communication networks require the estimation of the attenuation suffered by radio signals as they propagate between the transmitter and receiver in different environments. The International Telecommunications Union recommendation sector (ITU-R) provides models that can be used by network planners to guide the installation of base stations. The paper presents an overview of the model adopted in the recommendation ITU-R, P. 1411-10.

1. Introduction

In the World Radiocommunications Conference 2015, WRC15, seven frequency bands with different bandwidths from 1.6 to 10 GHz in the frequency range 24–86 GHz were identified for possible allocation for future 5G wireless networks. This has prompted several propagation studies across the world to derive path loss models for the envisaged deployment scenarios and to estimate wideband channel parameters such as *r.m.s.* delay spread to aid in the design of 5G networks (Keusgen et al., 2014; mmMagic Deliverable 2.2, 2017; Raimundo et al., 2018; Sun et al., 2016; Zhang et al., 2018; Zhang et al., 2018). Due to the spread across multiple bands with different bandwidths and the need to characterize the radio channel in these new bands in preparations for WRC 2019, a number of correspondence groups were formed in three of the working parties of Study Group 3 (SG3) of the International Telecommunications Union (ITU) which provides recommendations on radio wave propagation. Due to the high path loss and blockage in the identified frequency bands, three correspondence (CG) groups were set up to tackle different aspects of the radio channel. CG-3K-6 was set up within working party (WP) 3K to harmonize the path loss models over short urban paths in ITU-R recommendation P.1411. CG-3K-3M-12 was set up to predict clutter loss, jointly between WP 3K and WP 3M which deals with point-to-point and earth-space propagation. The third CG-3J-3K-3M-8 was set up between WP 3K, WP 3M, and WP 3J which deals with propagation fundamentals to model building entry loss.

In this paper, we give an overview of the work carried out by CG 3K-6 to derive the site general path loss model adopted in the recent Recommendation ITU-R P.1411-10 (2019) for two out of the five propagation environments classified in the recommendation. These are (i) *urban high rise* characterized with tall buildings of several floors each and (ii) *urban low rise/suburban* with wide streets and building heights with less than three stories making diffraction over roof top likely. Both line of sight (LOS) and non-LOS (NLOS) were measured for two distinct scenarios: (i) below the rooftop scenario where both stations are below the height

of the surrounding rooftops, where station refers to either the transmitter or the receiver and (ii) above the rooftop scenario, where one station is above the rooftops of neighboring buildings and the second station is below the rooftops.

In this paper, we start by describing the different measurement equipment including calibration procedures. This is followed by the methodology of data collection and data analysis to derive the path loss model.

2. Measurement Equipment and Environment

Three different types of equipment covering different frequency bands were used in the measurements. These include multiple band continuous wave (CW) transmissions and wideband measurements using either a dual band pseudo random binary sequence (PRBS) or frequency-modulated continuous wave sounder (FMCW, also known as chirp). The wideband sounders have varying bandwidths ranging from 250 MHz to 6 GHz and the measurements extended over different distances up to 1,200 m. In this section, we detail the equipment used in the measurements, the calibration procedures, and the measurement environment.

2.1. CW Measurements

CW measurements were carried out by two administrations with multiple bands. One set up covered three frequency bands: 6, 10, and 18 GHz, and the second set up five different frequency bands: 0.8, 2.2, 4.7, 26.4, 37.1, and 66.5 GHz. Figure 1 shows two of these setups which cover the frequency ranges from 0.8 to 66.5 GHz (Sasaki et al., 2015; Sasaki et al., 2016; Sasaki et al., 2017a; Sasaki et al., 2017b; Sasaki et al., 2018; Sasaki et al., 2018a; Sasaki et al., 2018b) .

Each transmitter and receiver were individually calibrated where the power output of each transmitter was verified via a power meter, and each receiver was connected to a calibrated signal generator to determine its dynamic range as illustrated in Figure 2. A high gain Low Noise Amplifier (LNA) was used with narrowband receivers for the detection of low power signals.

The setup was used to conduct measurements in two scenarios (Sasaki et al., 2018, 2017, 2017, 2015, 2018). For above the rooftop scenario shown in Figure 3, the transmitter was set up at 55 m above ground and the receiver at 2.5 m. For the 66.5 GHz measurements, the half power beam-width (HPBW) of the transmit antenna was 30° while it was 60° for the 2.2-, 4.7-, and 26.4-GHz bands. For all frequency bands, the receive antenna had an omni-directional radiation pattern.

For below the rooftop measurements, both the transmitter and receiver antennas were omni-directional with the transmit antenna set up at 10 m and the receive antenna at 2.5 m. The measured environments are shown in Figures 3a–3b where buildings with multiple stories (about 40-m high) were lined along the road with typical road width of about 30 m.

2.2. Wideband Measurement Equipment

Two waveforms were used in the wideband measurements: PRBS and FMCW. The PRBS sounders clock rates were either 250 or 500 MHz while the FMCW sounder had a programmable bandwidth with a maximum bandwidth of 6 GHz in the 50 to 75-GHz band and 3 GHz in the 25 to 30-GHz band.

The 500-MHz PRBS sounder used a sequence length of 4,095 with a 12,500 sliding-factor. Using different Radio Frequency (RF) up converters, it covered the 28-GHz band and the 38-GHz band with 29- and 21-dBm output power, respectively. Figure 4 displays the different modules used in the sounder, which also used a 3-D positioner to mount directional horn antennas while controlling the boresight of the antenna with an accuracy of 1° (Lee et al., 2016).

The sounder is calibrated from back to back (B2B) tests with calibrated attenuators as shown in Figure 5a and from on the air measurements. The resulting B2B impulse response of the sounder, is shown in Figure 5b which following equalization closely approximates the ideal impulse response with about 47-dB peak to noise ratio (Kwon et al., 2015).

To capture the effects of the antenna and cable connections, an open-area calibration along a straight-line road is conducted using an identical setup to that employed in the field measurements. Figure 6 shows that the calibrated open-area path loss follows the theoretical two-ray model where the discrepancies are attributed to the nature of the road in the open area (Lee et al., 2018).

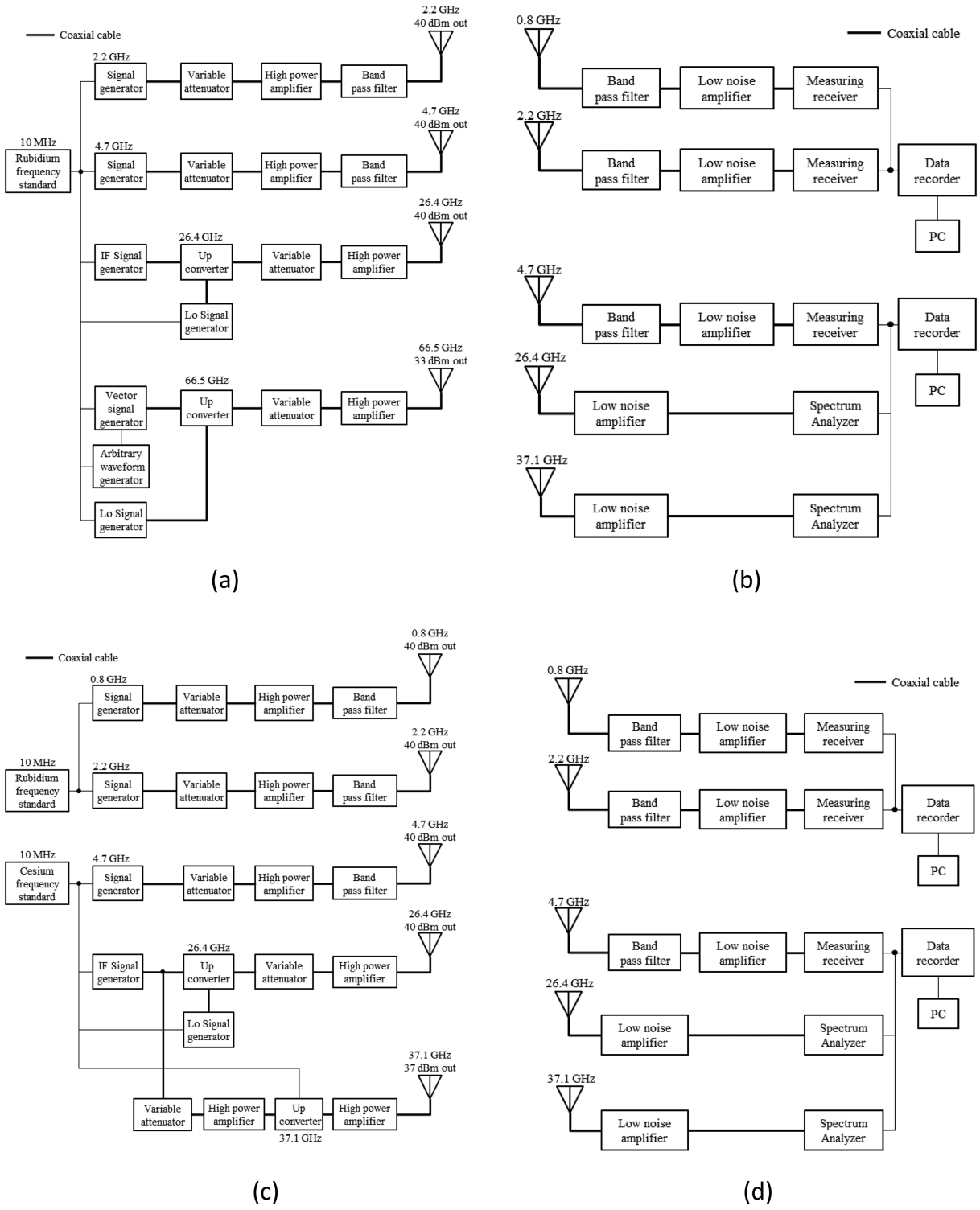

Figure 1. Transmitter (a) and (c) and receiver (b) and (d) configurations in the frequency bands 0.8 to 66.5 GHz.

The sounder was used in below the rooftop measurements in the urban high-rise environments of Figures 7a, 7b, and 7c and the urban low-rise environment in Figure 7d. The transmitter height was set either at 10 or 4 m while the receiver height was fixed at 1.5 m. The transmitter antenna with a 30° HPBW was pointed towards the receiver which used an omni-directional antenna. The data were either

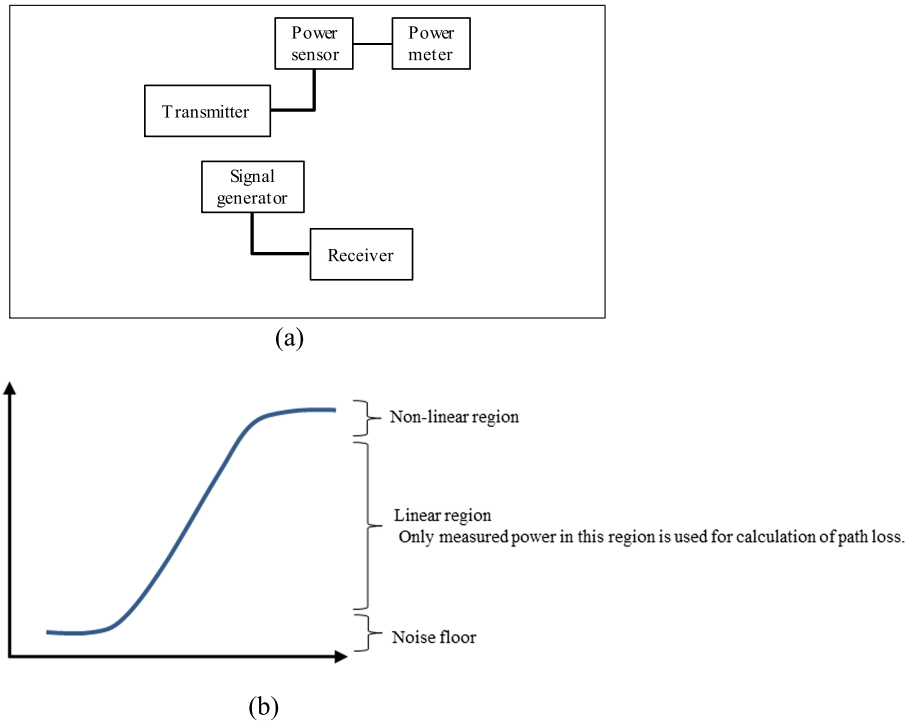

Figure 2. (a) Calibration setup of the transmitter and receiver. (b) Estimation of dynamic range of receiver.

collected continuously, or 30 samples were captured at each receiver point and the median value was taken to represent the path loss.

Similarly, the 250-MHz PRBS sounder which covered the 10- and 60-GHz bands was calibrated from B2B tests and open environment tests. The sounder was used to collect data in urban high-rise and suburban low-rise environments.

The FMCW sounder described in (Salous et al., 2016) was upgraded in order to cover additional frequency bands as identified by WRC15. This was achieved by a programmable local oscillator (ADF5355) as shown in Figure 8 to up convert the Intermediate Frequency (IF) signal in the 2.2–2.9 GHz band to the band

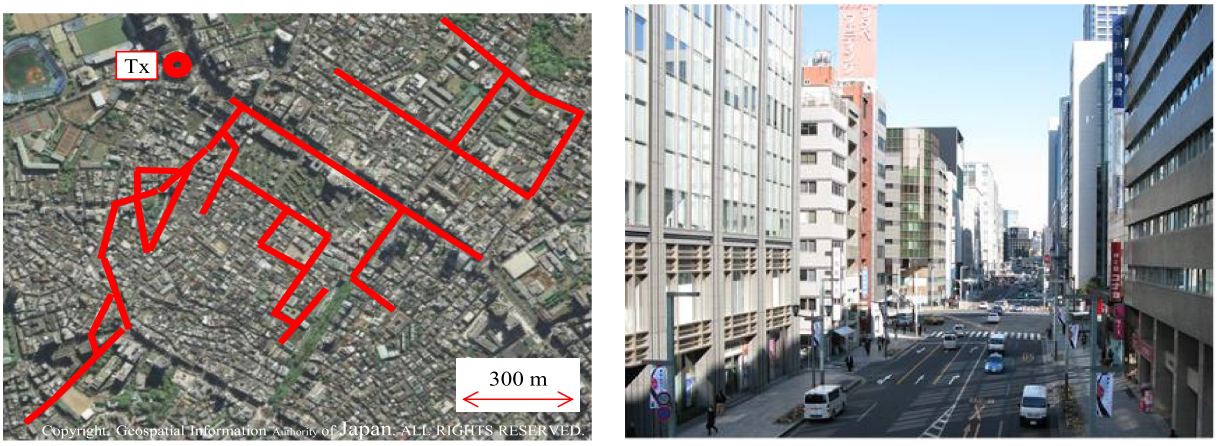

Figure 3. Environment for above the rooftop measurements. (a) Route of measurements and (b) typical environment.

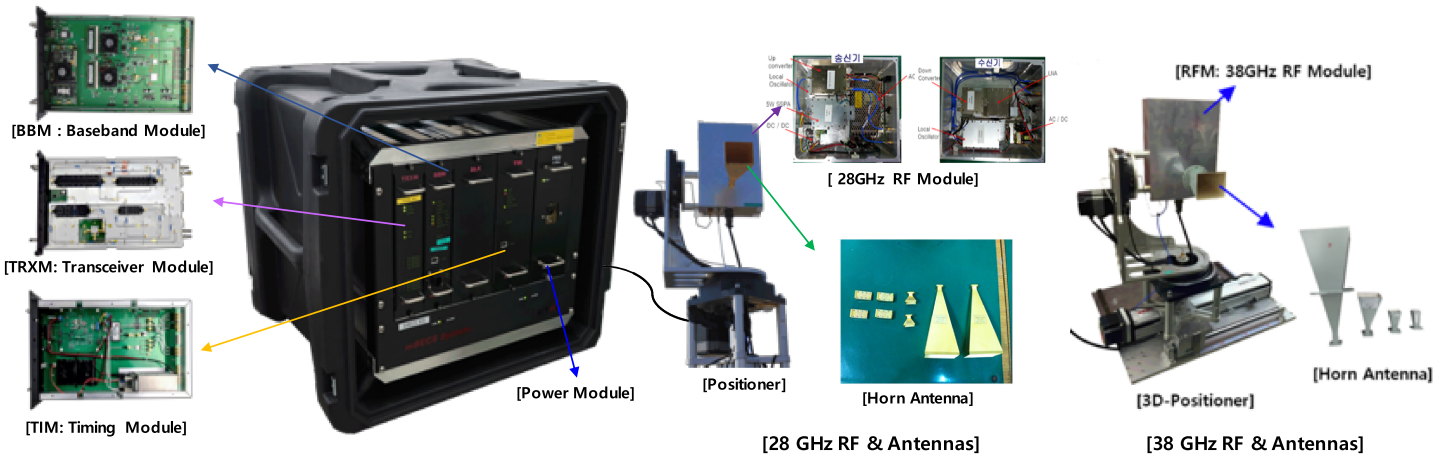

Figure 4. Pseudo random binary sequence sounder configuration for the 28- and 38-GHz bands.

between 12.34 to 18.2 GHz with a maximum bandwidth of 1.5 GHz. Using the new IF unit in conjunction with two RF heads as shown in Figure 9, three of the frequency bands identified by WRC15 are covered; the 25.5–28.5 GHz and 51–57 GHz bands were measured simultaneously, and the measurements were repeated for the 67–73 GHz band along the same route. At the transmitter a two-way switch was used to enable the switching between the two bands and using built in switches in the RF heads, horizontal and vertical polarizations were transmitted using directional antennas with 55° HPBW in the 50–75 GHz band and 33° for the 25- to 30-GHz band. The use of the additional switch at the transmitter enables the identification of the polarization at the transmitter by introducing an off period. Thus, for each band, the sequence of transmission was horizontal, vertical, and two off periods where each period corresponds to one sweep. At the receiver, omni-directional antennas were used for all the bands. The sounder was calibrated from B2B measurements and on the air measurements in an anechoic environment.

The sounder was used in suburban below the rooftop and above the rooftop, LOS, and NLOS measurements in the environment shown in Figure 10 with transmit antenna height either at 3 or 18.2 m, respectively, with the receiver antenna height being fixed at 1.6 m. Figure 11 displays an example of the power delay profile for the co-polar and cross polar transmission at 25.5–28.5 and 51–57 GHz in a LOS scenario. Data were collected continuously over 2 s every 1 min to provide consecutive spatial measurements.

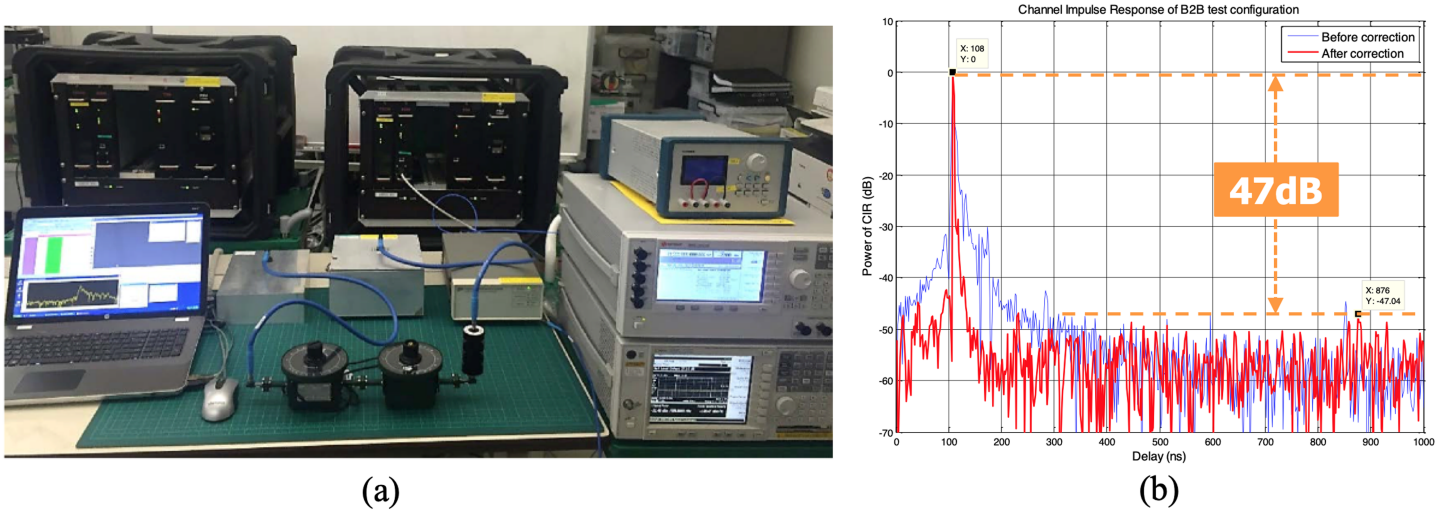

Figure 5. Back-to-back (B2B) calibration in a lab.

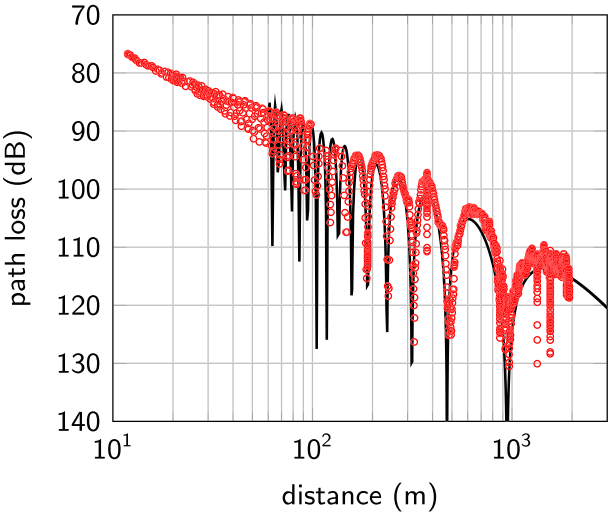

Figure 6. Open area measurements compared with the two-ray model.

Table 1 gives a summary of all the measured frequency bands, the type of transmission, the distance covered, and the propagation category.

3. Data Analysis and Derived Propagation Model

To derive the channel model for the categories defined in Recommendation ITU-R P.1411, it was necessary to identify a suitable path loss model approach as well as the spatial samples and the minimum signal to noise ratio to be used in the derivation of the model.

3.1. Model Approach

Several path loss models are proposed in the literature which are based either on a single frequency as in equation (1) or on multiple frequencies as in equation (2), where α and γ are the distance and frequency coefficients, d is the 3-D transmitter-receiver (T-R) separation distance in meters, f is operating frequency in GHz, and $N(0,\sigma)$ is a normal distribution with standard deviation equal to σ describing the large-scale variations of the path loss about the mean over distance. The value of β in dB can be either estimated from the measurements, or fixed to the free space

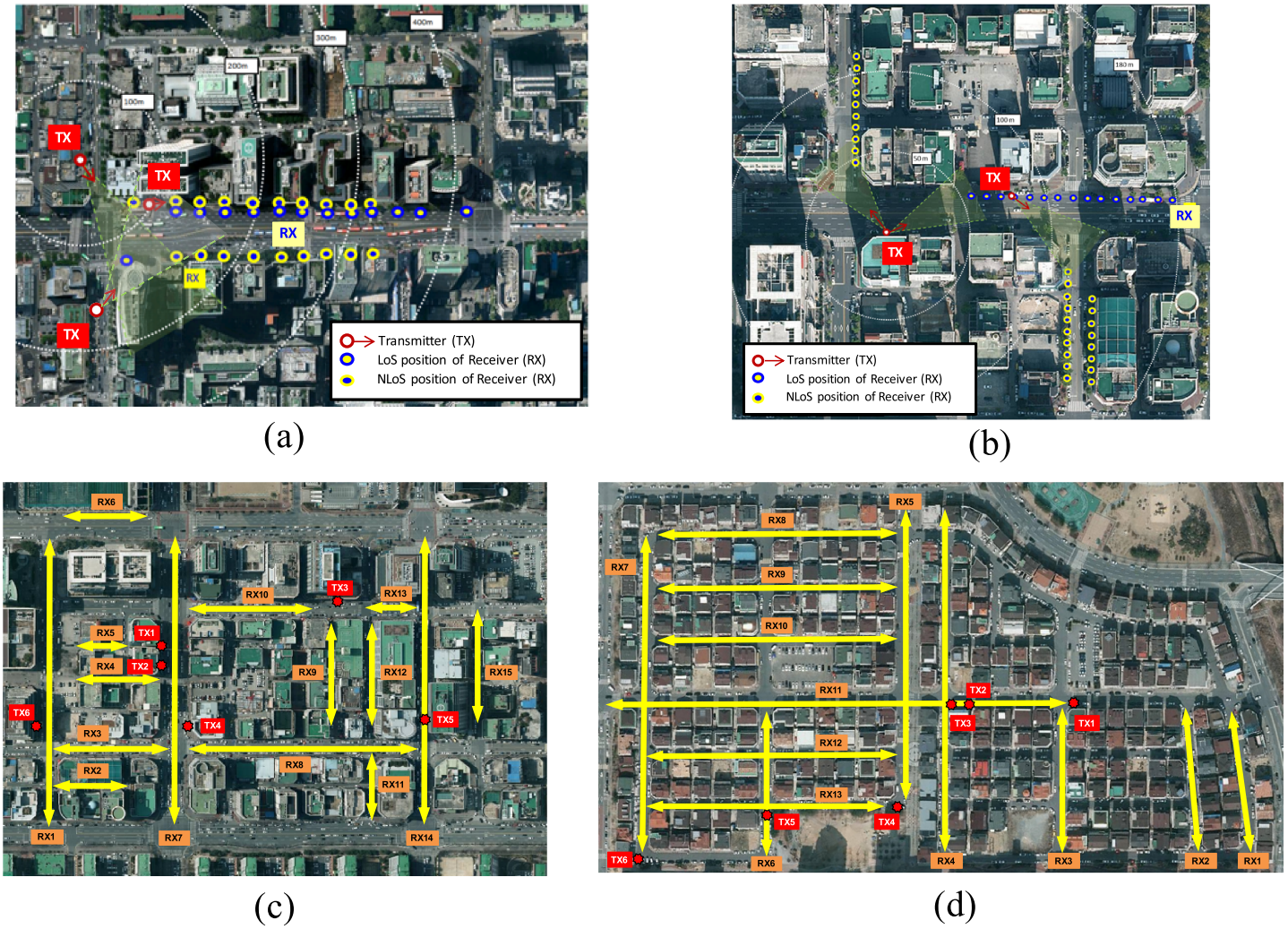

Figure 7. Measurement sites with the 500-MHz pseudo random binary sequence sounder (a–c) urban high rise and (d) urban low rise.

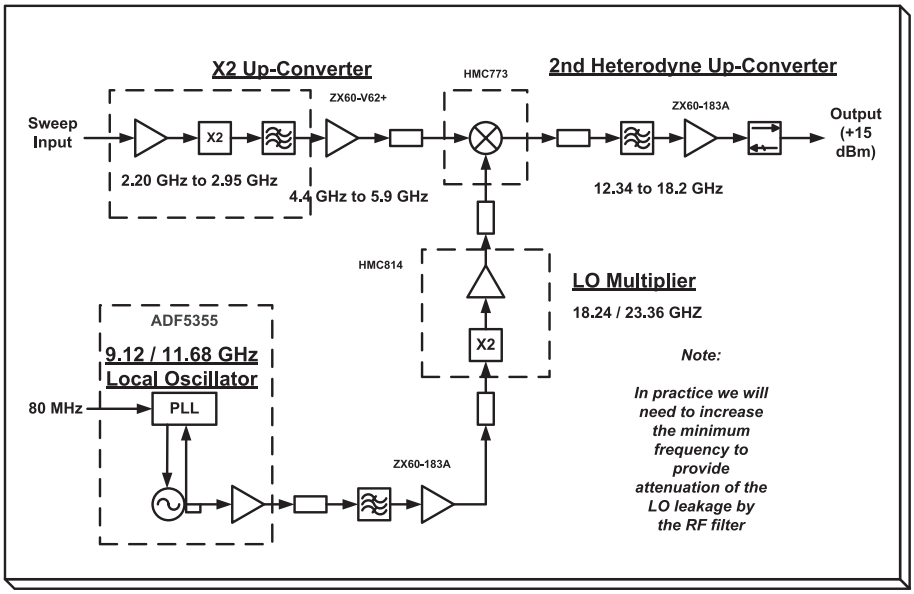

Figure 8. New IF unit with programmable Local Oscillator.

path loss at 1 m as in the close-in path loss model (Sun et al., 2016). The model in equation (2) is referred to as the alpha, beta, gamma model and can be used across a wide range of frequencies without the need for a different coefficient for each frequency band as in the alpha, beta model of equation (1).

$$PL_{logDist}(d) = 10\alpha\log_{10}(d) + \beta \; dB \tag{1}$$

$$PL(d,f) = 10\alpha\log_{10}(d) + \beta + 10\gamma\log_{10}(f) \; dB, \tag{2}$$

with an additive zero mean Gaussian random variable $N(0,\sigma)$ with a standard deviation σ (dB).

Since the measurements were collected over a wide frequency range from 0.8–73 GHz, the model in equation (2) was adopted as it provides a single set of four parameters and only requires distance and frequency.

3.2. Data Verification

Since the collected data had varying number of spatial data points and different waveforms were used in the measurements, it was necessary to identify a suitable approach for the estimation of path loss, minimum acceptable signal to noise ratio, and the spatial sampling of the data. For the wideband measurements, the data were analyzed to estimate the received power from the area under the power delay profile (PDP) as in Figure 11 following the procedure in Recommendation ITU-R P.1407-6 (2019). For the wideband measurements performed with the FMCW sounder, the data were processed with 2-GHz bandwidth for the PDPs

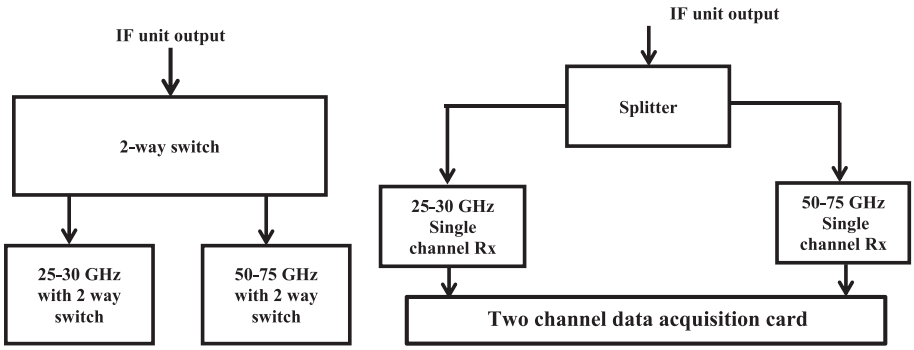

Figure 9. Block diagram of the dual band setup at the transmitter and receiver.

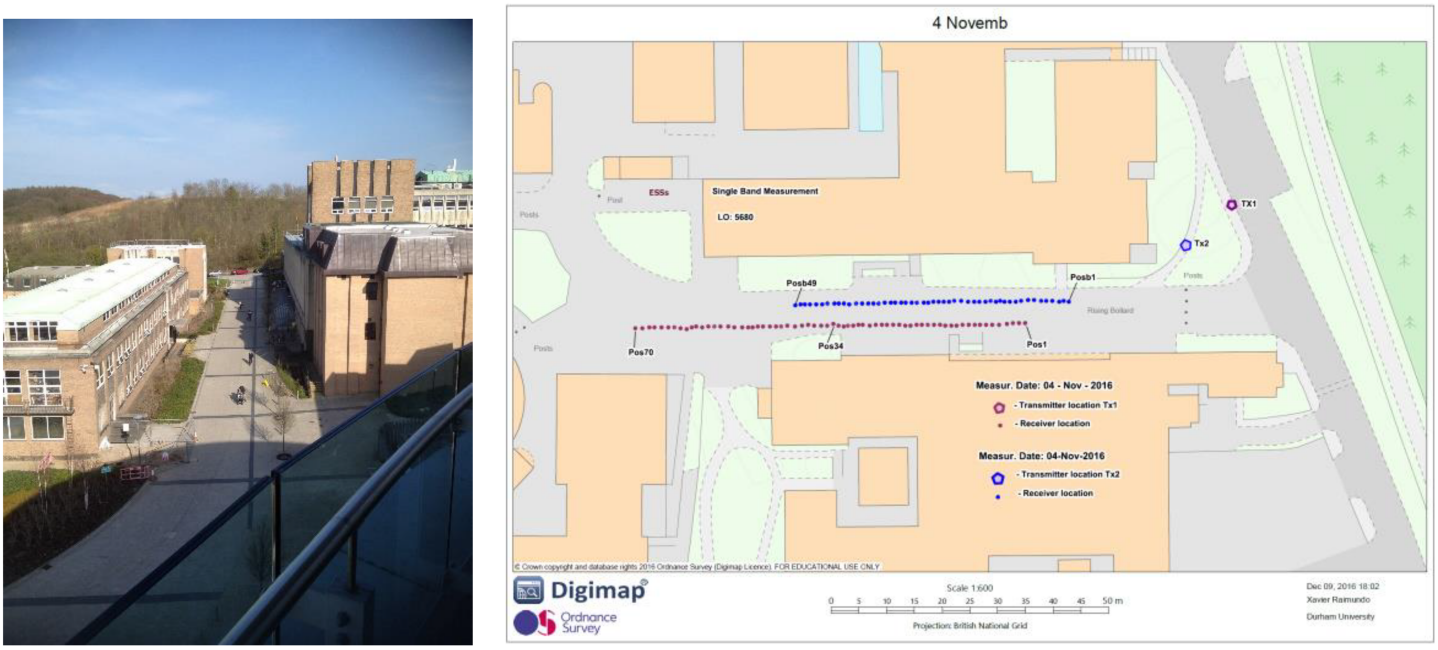

Figure 10. (a) Suburban measured environment and (b) one of the measured routes.

for all the three bands. For each meter of measurement, five power delay profiles were estimated by averaging 488 impulse responses giving a PDP every 20 cm. For each PDP, the noise floor mean was estimated, and a 3 dB above the mean noise was used to set a noise threshold to ensure that the computed received power did not include noise samples. For CW measurements, a sampling rate of 45 kHz was used giving about 4,000 points of data per meter. The distance between the transmitter and receiver antennas was calculated using global positioning system data.

Since the data sets were collected with different number of spatial samples and with different systems over varying distances, it was necessary to identify a suitable common number of samples per meter to avoid the model being biased by any particular data set as illustrated in Figure 12a which shows the collected data versus distance across the frequency band from 0.8–70 GHz for the LOS below rooftop environment. Two approaches were tested for the decimation of data. The average values or the median value every 1 m were computed from each data set, and the model parameters were estimated. No significant difference was detected in the two approaches and the local average at every 1 m was adopted in the model as illustrated in

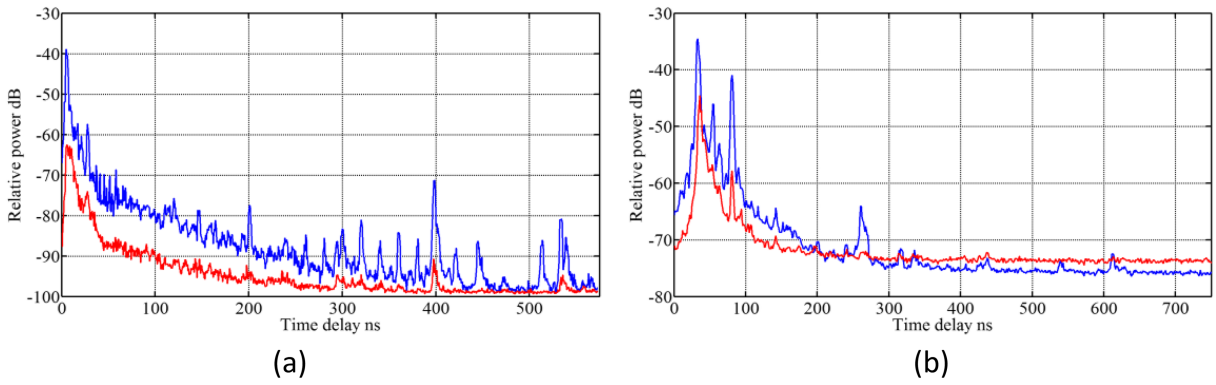

Figure 11. Power delay profile at (a) 25.5–28.5 GHz and (b) 51–57 GHz in line of sight scenario.

Table 1
Data Sets for the Development of the Site-General Models for Urban and Suburban Environments Below Rooftop and Above Rooftop

Propagation category	Environment	Link type	Frequency (GHz)	Distance (m)	Transmission
Below roof top	Urban high-rise	LOS	0.8, 2.2, 4.7, 6, 10, 18, 26.4, 37.1	10–660	CW
			28, 38	10–380	PRBS, 500-MHz bandwidth
			60	5–50	PRBS, 250-MHz bandwidth
		NLOS	0.8, 2.2, 4.7, 6, 10, 18, 26.4, 37.1	40–715	CW
			28, 38	25–235	PRBS, 500-MHz bandwidth
	Urban low-rise/Suburban	LOS	10, 60	10–210	PRBS 250-MHz bandwidth
			27	20–140	FMCW, 3-GHz bandwidth
			28, 38	10–250	PRBS, 500-MHz bandwidth
			54, 70	10–140	FMCW 6-GHz bandwidth
		NLOS	10, 60	10–165	PRBS 250-MHz bandwidth
			27	10–140	FMCW, 3-GHz bandwidth
			28, 38	30–250	PRBS, 500-MHz bandwidth
			70	10–170	FMCW 6-GHz bandwidth
Above roof top	Urban high-rise	LOS	2.2, 4.7, 26.4	155–1,140	CW
			66.5	170–340	CW
		NLOS	2.2, 4.7, 26.4	260–1,630	CW
	Urban low-rise/Suburban		66.5	260–340	CW
		LOS	27	55–145	FMCW 3-GHz bandwidth
			70	55–145	FMCW 6-GHz bandwidth

Abbreviations: CW = continuous wave, FMCW = frequency-modulated continuous wave, LOS = line of sight, NLOS = non-line of sight, PRBS = pseudo random binary sequence.

Figure 12b. Similarly, 10- and 15-dB signal to noise ratio thresholds were tested and a minimum signal to noise ratio of 10 dB was used for all the data sets. The data were also combined in different groups to identify the frequency range and distance for the estimation of the model parameters. Only vertical to vertical polarization data were used in the estimation of the model parameters as all the data sets except for the FMCW data were collected with single polarization.

The estimated model parameters for the different environments are given in Table 2 as given in ITU-R P 1411-10 tables 4 and 8.

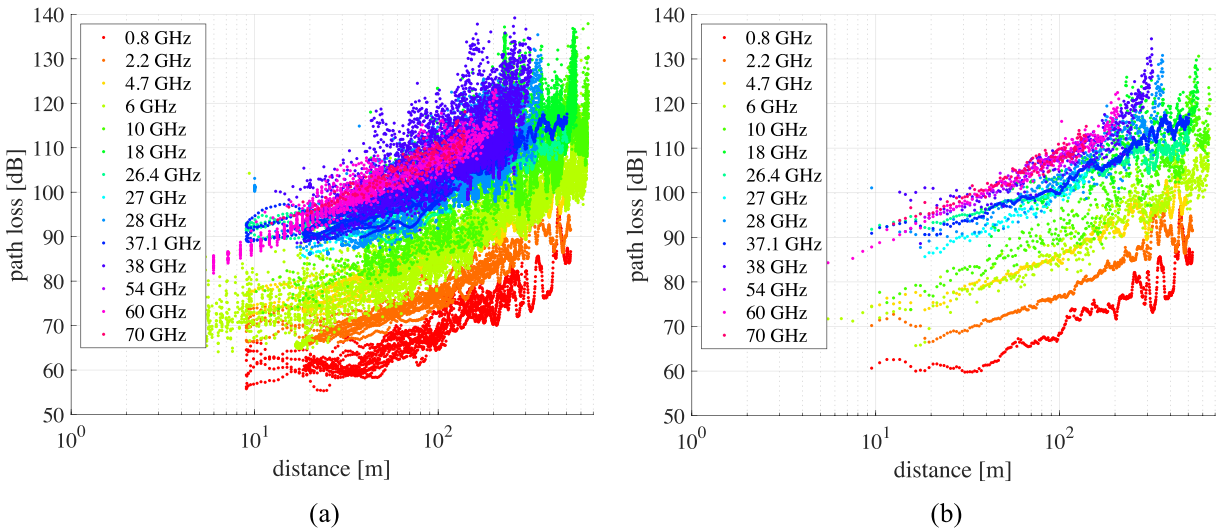

Figure 12. Path loss data versus distance (a) raw data and (b) decimated data with 1-m average

Table 2
Path Loss Coefficients Below Roof Top and Above Roof Top

Propagation category	Frequency range (GHz)	Distance range (m)	Type of environment	LOS/NLOS	α	β	γ	σ
Below-rooftop propagation	0.8–73	5–660	Urban high-rise, Urban low-rise/Suburban	LOS	2.12	29.2	2.11	5.06
	0.8–38	30–715	Urban high-rise	NLOS	4.00	10.2	2.36	7.60
	10–73	30–250	Urban low-rise/Suburban	NLOS	5.06	−4.68	2.02	9.33
Above-rooftop propagation	2.2–73	55–1,200	Urban high-rise, Urban low-rise/Suburban	LOS	2.29	28.6	1.96	3.48
	2.2–66.5	260–1,200	Urban high-rise	NLOS	4.39	−6.27	2.30	6.89

Abbreviations: LOS = line of sight, NLOS = non-line of sight.

4. Use of the Channel Model in Monte Carlo Simulations

In network design and sharing studies, Monte Carlo simulations are used to estimate the path loss from the model taking into account the standard deviation from the median value. Due to the high value of σ and the steeper slope of the NLoS model with respect to the free space deterministic path loss model, path loss values can be lower than free space as illustrated in Figure 13 at 70 GHz where the urban low rise/suburban model is shifted from the median by 1%, 5%, and 10% of σ in comparison to the free space path loss. The model gives values below free space loss for distances less than 80 m. Since the measurements did not have any values below free space path loss, a capping approach similar to Recommendation ITU-R P. 2109-0 (2019) model was investigated. The capping method limits the excess path loss with respect to free space loss, L_{FS}, such that no values generated in the simulation fall below free space.

This corresponds to the condition that the difference with respect to free space will not exceed $10\log_{10}(10^{0.1A}+1)$ (dB), where A is a random variable with a normal distribution, $N(\mu,\sigma)$, $\mu = PL(d,f) - L_{FS}$, $L_{FS} = 20\log_{10}(4\times10^{9}\pi df/c)$, and c is the speed of light in meters per second. The capping method is adopted in recommendation ITU-R P. 1411-10.

In Sun et al. (2016) values of path loss coefficients for the alpha, beta, gamma model are given for two scenarios' classified as UMa and UMi which refer to the transmit antenna height as either 25 m above rooftop or 10 m at rooftop. Therefore, according to this classification only the UMa results can be compared with the model reported in this paper. However, the values given in table 3 by Sun et al. (2016) cover the frequency range 2–38 GHz for distances 61–1,238 m, whereas the values presented in this paper cover the frequency range 2.2–66 GHz and for distances from 260 to 1,200 m. Similar classification of scenarios is also adopted

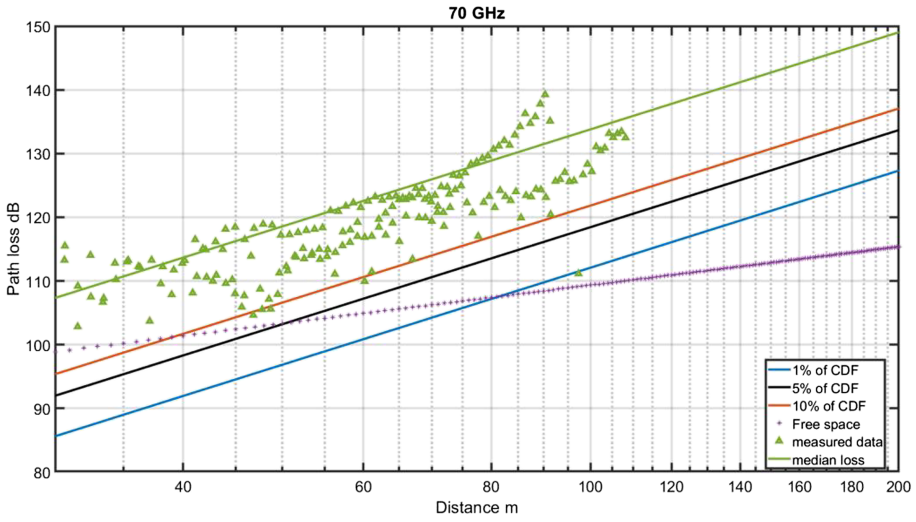

Figure 13. Path loss model for low-rise urban/suburban with different displacements ratios of σ with respect to free space loss. CDF=Cumulative Distribution Function.

in the more recent 3GPP report "3GPP TR 38.900V15.0.0 (2018-06)" which gives path loss models for frequency ranges from 6 to 100 GHz. For the NLoS UMa scenario, the model is given in equation (3) which has a correction factor for the user-terminal antenna height, h_{UT}, above 1.5 m. Assuming, that the user terminal antenna height is 1.5 m, the model gives values of 3.908 for alpha, 13.54 for beta, and 2 for gamma with sigma equal to 6 dB.

$$PL'_{UMa\text{-}NLOS} = 39.08\log_{10}(d_{3D}) + 13.54 + 20\log_{10}(f_c) - 0.6(h_{UT} - 1.5) dB \text{ for } 10m \leq d_{2D} \leq 5km \quad (3)$$

To avoid the path loss falling below free space, it limits the path loss to the maximum of $\left(PL'_{UMa-NLOS}, PL_{UMa-LOS}\right)$. This effectively leads to two different path loss coeffcicients; which is avoided in the capping method.

It also gives an optional model as given in equation (4), which assumes free space propagation for the value of alpha, a coefficient of 2 for frequency and has a value of 3 for alpha with sigma equal to 7.2 dB.

$$PL = 30\log_{10}(d_{3D}) + 32.4 + 20\log_{10}(f)\ dB \quad (4)$$

The model presented in this paper is the adopted ITU model in its Recommendation ITU-R P.1411-10 (2019) with the approved capping method which aims to provide a model appropriate for the scenarios as defined in the recommendation.

5. Conclusions

Measurements were performed in different environments in Japan, Korea, and the United Kingdom as classified by Recommendation ITU-R P.1411 to derive a suitable path loss model for 5G wireless networks. The measurements covered frequency ranges between 0.8 to 73 GHz with either narrowband or wideband sounders. Data were systematically collected over typical distances, and the data were classified as LOS and NLOS for below the rooftop and above the rooftop scenarios, and the model parameters were estimated. The model was adopted in Recommendation ITU-R P.1411-9 and the capping approach approved for future updating of the recommendation.

Acknowledgments
The work of J. Lee and M. D. Kim was supported by Institute for Information & Communications Technology Planning & Evaluation (IITP) grant funded by the Korean government (MIST) [2017-0-00066, "Development of time-space based spectrum engineering technologies for the pre-emptive using of frequency"]. The channel sounder at Durham University was developed under EPSRC project PATRICIAN EP/I00923X/1, and its frequency range extended under further funding from EPSRC Impact, Acceleration Account, Ofcom, UK, under contract 1362, "Long term measurements campaign and development of model(s) for mm wave bands (30–90 GHz)" and Intel, USA. Data in the 60 GHz band were provided by Intel, USA. Discussions with Correspondence Group 3K-6 of the ITU working party 3K and in particular Jonas Medbo on the capping method are appreciated. All the data used in the paper are summarized in Table 1. The data, except 0.8, 2.2, 4.7, 26.4, 37.1, and 66.5 GHz frequency data, are available at https://www.itu.int/md/R15-WP3K-C-0125/en which is an ITU-R contribution document accessible only, at this time, for those who have an ITU-R ties account. These data may or may not be publicly available subject to the ITU-R policy. The measurement data at frequencies 0.8, 2.2, 4.7, 26.4, and 37.1 GHz are not publicly available due to the current data policy of NTT Corporation.

References

3GPP TR 38.900 V15.0.0 (2018-06), Study on channel model for frequency spectrum above 6 GHz (Release 15)

Keusgen, W., Weiler, R. J., Peter, M., Wisotzki, M., Göktepe, B., (2014), Propagation measurements and simulations for millimeter-wave mobile access in a busy urban environment, 39th International Conference on Infrared, Millimeter, and Terahertz waves (IRMMW-THz).

Kwon, H.-K., M.-D. Kim and J. Liang, (2015), "Evaluation of multi-path resolution for millimetre wave channel sounding system," Proc. Int. Conf. ICT Convergence (ICTC), pp. 1037–1039, Jeju Korea.

Lee, J., Kim, M. D., Park, J. J., & Chong, Y.,. J. (2018). Field-measurement-based received power analysis for directional beamforming millimetre-wave systems: Effects of beamwidth and beam misalignment. *ETRI Journal*, *40*(1), 26–38.

Lee, J., Liang, J., Kim, M. D., Park, J. J., Park, B., & Chung, H. K. (2016). Measurement-based propagation channel characteristics for millimetre-wave 5G Giga communication systems. *ETRI Journal*, *38*(6), 1031–1041.

mmMagic Deliverable D2.2, (2017), Millimeter-wave based mobile access network for fifth generation integrated communications, "measurement results and final channel models for preferred suitable frequency ranges. https://bscw.5g-mmmagic.eu/pub/bscw.cgi/d202656/mmMAGIC_D2-2.pdf

Raimundo, X., Salous, S., & Cheema, A. A. (2018). Indoor dual polarised radio channel characterisation in the 54 and 70 GHz bands. *IET Microwaves, Antennas & Propagation*, *12*(8), 1287–1292. https://doi.org/10.1049/iet-map.2017.0711

Recommendation ITU-R P.1407-6 (2019-08), Multipath propagation and parameterization of its characteristics.

Recommendation ITU-R P.1411-10 (2019-08), Propagation data and prediction methods for the planning of short-range outdoor radio-communication systems and radio local area networks in the frequency range 300 MHz to 100 GHz.

Recommendation ITU-R P.2109-0 (2019-08), Prediction of building entry loss.

Salous, S., Feeney, S. M., Raimundo, X., & Cheema, A. A. (2016). Wideband MIMO channel sounder for radio measurements in the 60GHz band. *in IEEE Trans. on Wireless Communications*, *15*(4), 2825–2832. https://doi.org/10.1109/TWC.2015.2511006

Sasaki, M., M. Inomata, W. Yamada, N. Kita, T. Onizawa and M. Nakatsugawa, (2016), "Path loss characteristics`at multiple frequency bands from 0.8 to 37 GHz in indoor office," 10th European Conference on `Antennas and Propagation (EuCAP), Davos, pp. 1-4.

Sasaki, M., Inomata, M., Yamada, W., Kita, N., Onizawa, T., Nakatsugawa, M., et al. (2018a). Path `Loss model considering blockage effects of traffic signs up to 40 GHz in urban microcell `environments. *IEICE Trans. on Commun.*, *E101-B*(8), 1891–1902.

Sasaki, M., Inomata, M., Yamada, W., Kita, N., Onizawa, T., Nakatsugawa, M., et al. (2018b). Frequency dependency of path loss between different floors in an indoor office environment at `UHF and SHF bands. *IEICE Trans. on Commun.*, *E101-B*(2), 373–382.

Sasaki, M., M. Nakamura, M. Inomata, W. Yamada, N. Kita, K. Kitao, et al., (2017a), `"Frequency dependence of path loss with wide dynamic range in urban macro cells between 2 and 26 GHz," IEEE Globecom Workshops (GC Wkshps), Singapore, pp. 1-6.

Sasaki, M., M. Nakamura, M. Inomata, W. Yamada, N. Kita, Y. Takatori, et al., (2017b) "Frequency `dependence of site-specific path loss in urban macro cell environments between 2 and 66 GHz bands," `IEEE 28th Annual International Symposium on Personal, Indoor, and Mobile Radio Communications ` (PIMRC), Montreal, QC, pp. 1-5.

Sasaki, M., M. Nakamura, W. Yamada, N. Kita, Y. Takatori, M. Inomata, et al.,(2018), "Pathloss characteristics from 2 to 66 GHz in urban macrocell environments based on analysis using ITU-R site-`general models," 12th European Conference on Antennas and Propagation (EuCAP), London, pp. 1-5.

Sasaki, M., Yamada, W., Sugiyama, T., Mizoguchi, M., & Imai, T. (2015). "Path loss characteristics at 800 MHz to 37 GHz in urban street microcell environment,"9th European Conference on Antennas and Propagation (EuCAP). *Lisbon*, *2015*, 1–4.

Sun, S., Rappaport, T. S., Thomas, T. A., Ghosh, A., Nguyen, H. C., Kovács, I. Z., et al. (2016). Investigation of prediction accuracy, sensitivity, and parameter stability of large-scale propagation path loss models for 5G wireless communications. *IEEE Transactions on Vehicular Technology*, *65*(5), 2843–2860.

Zhang, G., Saito, K., Fan, W., Cai, X., (2018), Panawit Hanpinitsak; Jun-Ichi Takada; Gert Frølund Pedersen, Experimental characterization of millimeter-wave indoor propagation channels at 28 GHz, IEEE Access, vol (6), pp 76516-7652

Zhang, P., Li, J., Wang, H., Wang, H., & Hong, W. (2018). Indoor small-scale spatiotemporal propagation characteristics at multiple millimeter-wave bands. *IEEE Antennas and Wireless Propagation Letters*, *17*(12), 2250–2254.